Cardiac Microlesions Form During Severe Bacteremic *Enterococcus faecalis* Infection

Armand O. Brown[1], Kavindra V. Singh[2], Melissa R. Cruz[1], Karan Gautam Kaval[1], Liezl E. Francisco[3], Barbara E. Murray[1,2], and Danielle A. Garsin[1*]

[1]Department of Microbiology and Molecular Genetics, The University of Texas Health Science Center at Houston, Houston TX, USA

[2] Division of Infectious Diseases, Department of Internal Medicine, The University of Texas Health Science Center at Houston, Houston, TX, USA

[3] Department of Biochemistry and Structural Biology, The University of Texas Health Science Center at San Antonio, San Antonio, TX, USA

*Corresponding author

Email: Danielle.A.Garsin@uth.tmc.edu

Abstract

Enterococci, such as *Enterococcus faecalis,* are a significant cause of hospital-acquired bacteremia and mortality among the elderly and patients with comorbid conditions in the healthcare setting. In this study, the novel discovery is made that cardiac microlesions form during severe bacteremic *E. faecalis* infection in mice. The cardiac microlesions were identical in appearance to those previously observed to form by *Streptococcus pneumoniae* during invasive pneumococcal disease (IPD) in mice, non-human primates, and humans. However, *E. faecalis* does not encode the virulence determinants implicated in pneumococcal microlesion formation, suggesting that formation is through an alternative pathway. In previous work, we showed that *E. faecalis* DsbA is required for the post-translational disulfide bond formation and stability of EntV, a secreted *E. faecalis* bacteriocin. Here, the role of DsbA in *E. faecalis* pathogenicity was explored. DsbA was discovered to be required for *E. faecalis* virulence in a *C. elegans* model and, importantly, was necessary for efficient cardiac microlesion formation. By investigating the cardiac host response, it was discovered that *E. faecalis* promotes cardiomyocyte necroptotic cell death at sites of microlesion formation. Additionally, by examining the cytokines induced by exposure of *E. faecalis* to cardiomyocytes, it was revealed that loss of DsbA caused a pro-inflammatory response unlike the wild type strain, which suppressed the immune response. In conclusion, we establish that *E. faecalis* is capable of forming cardiac microlesions and identify features of both the bacterial and host responses that are mechanistically involved.

62 **Significance Statement**

63

64 *E. faecalis* is a bacterium capable of causing serious disease in humans, including endocarditis,
65 an infection on the surface of the heart valves with a high mortality rate. In this work, we document
66 for the first time that *E. faecalis* is capable of also causing an invasive infection of the heart,
67 forming cardiac microlesions in a mouse model of severe bloodstream infection. Additionally, a
68 contributing bacterial factor is identified and the immune response of heart cells to infection with
69 *E. faecalis* is characterized. Overall, this work makes a significant contribution to the field of
70 infectious diseases by identifying a new enterococcal disease pathology, cardiac microlesion
71 formation, which was previously known to occur only with IPD.

72

73 **Introduction**

74

75 *Enterococcus faecalis* is a Gram-positive bacterium that normally co-exists with the host as a
76 harmless commensal. However, it is capable of causing a variety of infections such as infective
77 endocarditis (IE), urinary tract infection (UTI), bacteremia, peritonitis, prosthetic joint infection, and
78 endophthalmitis. These infections can become life-threatening if left untreated (1, 2). Furthermore,
79 immunocompromised individuals and those with underlying disease are at an increased risk (3-
80 5). Enterococcal infections are increasingly characterized by the presence of antimicrobial
81 resistance such as vancomycin resistant enterococci (VRE). Due to their intrinsic ability to survive
82 various environmental habitats (3), the bacterium poses a significant threat in hospitals and long-
83 term care facilities where VRE has increased access to immunocompromised patients through
84 infection of open wounds, or through the use of contaminated medical devices (6, 7). As such,
85 enterococci are a common nosocomial pathogen, having been observed to be the etiological
86 agent responsible for 14% of all hospital-acquired infections (HAIs) in the US between 2011–2014
87 (8). Therefore, it is no surprise that enterococci are a significant cause of hospital-acquired
88 bacteremia and mortality among the elderly and patients with comorbid conditions in the
89 healthcare setting (9-12).

90

91 Enterococcal infections often lead to other clinical manifestations. A common complication
92 associated with bacteremia is endocarditis, an infection that has a 1-year mortality rate of
93 approximately 29% despite antibiotic therapy (11). Enterococci are the third most common cause
94 of endocarditis in North America (5) and, in patients with this infection, heart failure has been
95 observed to occur with increased frequency (13-19). Infective endocarditis involves the formation
96 of biofilms on heart valves and inner chambers that develop into complex masses called
97 vegetations (2). Thus, heart infections associated with *E. faecalis* have traditionally been

98 characterized as occurring on the surfaces of the heart, rather than in the deeper myocardial
99 tissue, which would require active invasion by the bacterium.
100
101 Interestingly, another important Gram-positive pathogen, *Streptococcus pneumoniae,* was
102 recently shown to invade the heart tissue and form cardiac microlesions during invasive
103 pneumococcal disease (IPD) (20). The microlesions occurred in mice, non-human primates, and
104 humans with IPD and were shown to be associated with altered cardiac electrophysiology, heart
105 failure in mice, and scar formation during convalescence (20). Scar formation following
106 microlesion development is thought to predispose individuals to major adverse cardiac events
107 (MACE) (21). Moreover, cardiac microlesions were shown to form following vascular endothelial
108 cell invasion into the myocardial tissue, followed by subsequent interactions between
109 pneumococcal Choline binding protein A (CbpA) and pneumococcal teichoic acid associated
110 phosphorylcholine (ChoP) with host laminin receptor (LR) and platelet activating factor receptor
111 (PAFr), respectively. Furthermore, cardiomyocyte death is mediated by exposure to the
112 pneumococcal secreted cholesterol-dependent pore forming toxin, pneumolysin (20, 21), and
113 hydrogen peroxide (22, 23). As such, cardiac microlesions have been proposed to be a
114 contributory factor to the onset of MACE observed in older patients with IPD, or in convalescent
115 patients previously hospitalized with IPD (20, 24, 25). Importantly, invasive infection is now
116 appreciated as a risk factor for myocardial infarction, and the risk appears to be more pronounced
117 depending on the severity of the infection (26, 27). Since the original observation of pneumococcal
118 microlesions in 2014, no other organism has been observed to cause such pathology.
119
120 In this report, we show that cardiac microlesions also form during invasive *E. faecalis* infection.
121 The observed cardiac microlesions are identical in appearance and size to *S. pneumoniae*
122 mediated cardiac microlesions, are diffuse across the myocardium, and are characterized by an

123 absence of immune cell infiltration. Furthermore, we identify a mode of cardiomyocyte cell death,
124 and an enterococcal determinant required for microlesion formation. Our findings suggest a
125 previously unrecognized pathological aspect of enterococcal infection that may be a contributing
126 factor to the increased rate of heart failure and mortality observed in patients with endocarditis
127 (13-19). Importantly, because *E. faecalis* lacks homologs of the virulence determinants previously
128 implicated in pneumococcal microlesion formation, the mechanism of microlesion formation for *E.*
129 *faecalis* is likely through an alternative pathway.
130
131

132 **Results**

133

134 **Cardiac microlesions form during severe bacteremic *E. faecalis* infection.** In previous work,
135 we implicated a previously uncharacterized *E. faecalis* thioredoxin known as DsbA (disulfide bond
136 forming protein A) as a requirement for the stability of EntV, a secreted bacteriocin that we
137 determined inhibits hyphal morphogenesis of the human fungal pathogen *Candida albicans* (28,
138 29). To test if these proteins had any effects on the fitness and pathogenicity of *E. faecalis*, we
139 infected *Caenorhabditis elegans* with *ΔdsbA* and *ΔentV E. faecalis* mutants and measured
140 survival. As shown in Figure 1A, loss of *dsbA* significantly attenuated mortality in infected
141 nematodes. Note that the *ΔdsbA* mutant did not manifest different growth kinetics when grown in
142 culture medium compared to wild type, ruling out a general growth defect (Figure S1). Infection
143 with the complement, *ΔdsbA::dsbA*, partially rescued the *ΔdsbA* phenotype. The partial
144 complementation was attributed to the DsbA protein being produced at lower levels in the
145 complemented strain (Figure 1B). No significant difference in nematode survival was observed
146 following infection with either the *ΔentV* mutant or its complement (Fig. 1A). Considering that EntV
147 is the only known substrate of *E. faecalis* DsbA, the results suggest that DsbA has additional
148 targets that affect pathogenicity.

149

150 Based on these results, we wanted to know if loss of DsbA also affected virulence in a vertebrate
151 animal model of *E. faecalis* infection. Therefore, the mutants were tested in a mouse model in
152 which animals were injected intra-peritoneally with *E. faecalis* resulting in generalized bacteremia
153 leading to mortality. Significant survival differences between the mice infected with the different
154 strains were not observed. However, various organs were collected in order to determine if *E.*
155 *faecalis* infection induced any strain-specific, pathological effects. To our surprise, cardiac
156 microlesions were discovered within the myocardium that were devoid of immune cell infiltrate

157 (Fig. 2 A, B). The microlesions appeared to form within roughly the same time frame (~24 h.p.i.)
158 as cardiac microlesions that have previously been reported to occur during invasive infection with
159 *S. pneumoniae*, the only other pathogen known to cause cardiac microlesions to date (20).
160
161 *S. pneumoniae* mediated microlesions have been shown to form in mice, non-human primates,
162 and humans, and were correlated with heart failure in mouse models of infection (20). Because
163 *E. faecalis* lacks homologs of the pneumococcal virulence determinants identified to promote
164 pneumococcal cardiac microlesion formation, such as choline binding protein A (CbpA) (20), the
165 cholesterol-dependent pore forming toxin pneumolysin (20), and hydrogen peroxide (30), we
166 decided to study this phenomenon more closely. To verify that the observed microlesions were
167 the result of infection by *E. faecalis*, immunofluorescent staining on paraffin embedded cardiac
168 tissue sections from mice infected with *E. faecalis* with a polyclonal anti-enterococcal IgG antibody
169 was performed and revealed the presence of dense aggregates of *E. faecalis* within the
170 microlesions (Fig. 2C). The presence of bacterial DNA was further verified by DNA counterstaining
171 with DAPI that revealed an accumulation of non-cardiomyocyte nuclear DNA within microlesions
172 (Fig. 2D). To determine the contribution of DsbA toward microlesion formation, cardiac
173 microlesions found on hematoxylin and eosin stained paraffin embedded cardiac sections were
174 quantified following infection with Δ*dsbA*. From these experiments, a significant attenuation in
175 microlesion formation during infection with *ΔdsbA* was observed relative to wild type, while no
176 significant difference was observed in mice infected with the *dsbA* complement (Fig. 2E).
177 Furthermore, when the sizes of the cardiac microlesions were compared, the wild-type lesions
178 were significantly larger than those found in the Δ*dsbA* infected mice (Fig. 2F). Importantly, the
179 size of the microlesions appeared to correlate with level of *dsbA* expression observed in Western
180 blots of *E. faecalis* whole cell lysates (Fig. 1B), with the *ΔdsbA::dsbA* strain manifesting an in-
181 between phenotype to that of the *ΔdsbA* and wild-type strains, consistent with partial

182 complementation. In conclusion, these data demonstrate that cardiac microlesion formation
183 occurs during systematic infection with *E. faecalis* and is dependent on DsbA. Thus, for the first
184 time, loss of DsbA in *E. faecalis* is shown to affect pathogenicity in animal models of infection,
185 both invertebrate (*C. elegans*) and vertebrate (mice).
186
187 **Necroptosis contributes to cardiomyocyte cell death within microlesions.** In previous
188 studies of pneumococcal cardiac microlesion formation, apoptosis was found to be associated
189 with microlesion formation in mice (22). A subsequent study determined that cardiomyocyte cell
190 death occurs following exposure to pneumolysin (*ply*) and pneumococcal derived hydrogen
191 peroxide (*spxB*) (23). Based on these observations and the fact that *E. faecalis* lacks *ply* and *spxB*
192 homologs, we sought to determine whether *E. faecalis* could promote cell death of
193 cardiomyocytes and identify the mechanism. First, HL-1 cardiomyocytes were infected with *E.*
194 *faecalis* and subsequently lactate dehydrogenase (LDH) release into the cell culture supernatant
195 was measured to assess cell death. From these experiments, it was concluded that *E. faecalis*
196 induces cell death of cardiomyocytes. Furthermore, infection with a *ΔdsbA* mutant resulted in a
197 significant decrease in cardiomyocyte cell death (Fig. 3B), suggesting DsbA is required to
198 modulate this process. Since cardiomyocyte cell death was observed following exposure to *E.*
199 *faecalis*, we wanted to identify the mechanism. To test this question, an annexin V apoptosis and
200 necrosis assay was performed to determine if *E. faecalis* promotes apoptosis or necrosis during
201 cardiomyocyte infection. The signals for both apoptosis and necrosis increased concomitantly
202 with time (Figure S2), and this read-out means that cell death is occurring by an apoptosis-
203 independent mechanism (see Materials and Methods). One apoptosis-independent cell death
204 pathway is necroptosis, and this mechanism of cell death is consistent with data published by
205 investigators studying *S. pnuemoniae* microlesions, which showed that markers of necroptosis
206 could be detected within the myocardium of acutely ill mice (20) and non-human primates (21).

207 Importantly, necroptosis is considered a key cell death pathway in cardiomyocytes during
208 ischemia-reperfusion injury and acute coronary syndrome (31-33). To test the hypothesis that
209 cardiomyocytes undergo necroptosis following exposure to *E. faecalis*, we infected HL-1
210 cardiomyocytes with this bacterium in the presence of various inhibitors of necroptosis and
211 observed a significant suppression of cell death (Fig. 3C). Additionally, staining for markers of
212 necroptosis (34), such as mixed lineage kinase domain-like pseudokinase (MLKL) and
213 phosphorylated MLKL, on cardiac tissue sections obtained from infected mice showed
214 concentrated signals within the microlesions (Fig 3D). Despite the ability of *E. faecalis* to promote
215 death of the cardiomyocytes following exposure, antibiotic protection assays indicated that the
216 bacteria were unable to invade cardiomyocytes relative to endothelial cells (Fig. 3A). No difference
217 was observed in either the ability to promote necroptosis or cell invasion following exposure to
218 *ΔdsbA* relative to wild-type (Figure S3). Taken together, these results suggest that during
219 bacteremia, *E. faecalis* is able to translocate across the vascular endothelium in order to enter
220 the myocardial tissue. Once there, *E. faecalis* is unable to invade cardiomyocytes, but can form
221 microcolonies that promote necroptotic cell death.

222 **Cardiomyocyte inflammatory cytokine response is suppressed following exposure to *E.***
223 ***faecalis*.** Cardiac microlesions are characterized by bacteria filled vacuoles that are largely devoid
224 of immune cell infiltrate (20, 30). Therefore, this pathology was distinguished from myocardial
225 abscesses, commonly caused by *Staphylococcus aureus*, which are suppurative infections
226 characterized by a robust immune cell infiltrate within the cardiac tissue (20, 35). Previous efforts
227 to explain the lack of an immune response to pneumococcal microlesions have yielded interesting
228 insights. For example, *S. pneumoniae* within microlesions are thought to subvert the host
229 response through a biofilm-mediated mechanism involving the pneumolysin mediated killing of
230 resident macrophages, thus creating a more permissive environment for pneumococcal growth
231 and survival (22). There are also examples of *E. faecalis* subverting the immune response. In

232 previous work, it was shown that *E. faecalis* can survive within mouse peritoneal macrophages
233 for extended periods of time enabling the bacteria to replicate and spread (36). In more recent
234 work, *E. faecalis* was shown to activate Phosphatidylinositol 3-Kinase signaling that inhibits
235 apoptosis (37). *E. faecalis* can also resist phagosome acidification and autophagy within
236 macrophages (38). Because *E. faecalis* does not encode a pneumolysin homolog, nor does it
237 secrete toxins known to kill macrophages or other immune cells, we wanted to examine the
238 immune response to *E. faecalis* within the heart by measuring various inflammatory cytokines and
239 chemokines. Experiments assessing cardiomyocyte inflammatory chemokine and cytokine levels
240 showed that wild-type *E. faecalis* promotes an immune quiescent response, while loss of *dsbA*
241 leads to a more inflammatory immune response (Fig. 4A). Interestingly, EGF, M1P-1a, GM-CSF,
242 IL-6, G-CSF, and INFr were significantly upregulated during infection with ***Δ****dsbA* relative to the
243 wild-type infected cardiomyocytes. Thus, these results implicate the contribution of specific host
244 signaling pathways involved in pathogen clearance that are normally suppressed in the presence
245 of DsbA during infection, as modeled in Figure 4B. Collectively, these data suggest that *E. faecalis*
246 inhibits a vigorous cardiomyocyte immune response in a manner similar to that of *S. pneumoniae*
247 despite lacking the components that *S. pneumoniae* uses during immune subversion. Future
248 studies will be focused on understanding the cardiomyocyte immune response during
249 enterococcal infection, and how DsbA contributes.

250

251 **Discussion**

252

253 In this work, we demonstrated for the first time that cardiac microlesions form during severe *E.*
254 *faecalis* bacteremic infection of mice. Importantly, microlesions occur despite *E. faecalis* not
255 encoding homologs of the pneumococcal virulence determinants implicated in microlesion
256 formation. These data suggest that *E. faecalis* may be expressing functionally redundant proteins
257 that serve to promote similar interactions to *S. pneumoniae* in mediating microlesion formation,
258 such as CbpA and pneumolysin, which facilitate vascular endothelial cell translocation and
259 cardiomyocyte cell death, respectively. Indeed, while *E. faecalis* does not encode a CbpA
260 homolog, it does encode other proteins capable of binding host extracellular matrix proteins.
261 These include EfbA, which binds fibronectin (39), ACE, which binds laminin receptor (40), and
262 Ebp pili that bind fibrinogen (41).

263

264 Interestingly, we did discover one factor, DsbA, that contributes to microlesion formation and
265 inhibition of the cardiomyocyte inflammatory immune response, as modeled in Figure 4B. Dsb
266 proteins work to catalyze disulfide bond formation in proteins and have been best studied in Gram-
267 negative bacteria where they catalyze the oxidative folding of proteins in the periplasm (42, 43).
268 In Gram-positive bacteria, oxidative protein folding of proteins targeted for the cell envelope or
269 secretion is thought to occur in the exoplasm, the area immediately outside of the cytoplasmic
270 membrane but before the peptidoglycan layer (42). While Dsb proteins and oxidative protein
271 folding have established importance in the biology of certain Gram-positive bacteria, like the
272 Actinomyces, Dsb proteins are not well studied in Firmicutes like *E. faecalis* and have generally
273 not been considered important (42). Most of these species secrete few proteins containing
274 cysteines and some, notably *S. pneumoniae*, do not encode any thiol-disulfide oxidoreductases
275 (44, 45). A deletion of the only DsbA-like protein in *S. aureus* resulted in no significant phenotypes

276 including no effects on pathogenicity (46). However, the discovery in this work that loss of DsbA
277 in *E. faecalis* profoundly affected pathogenicity in the *C. elegans* model and reduced cardiac
278 microlesion formation in the mouse sepsis model suggests that the lack of Dsb-related
279 phenotypes in *S. aureus* does not necessarily apply to all Firmicutes. It will be of interest to further
280 investigate the role of Dsb proteins in these species.
281
282 Because of the well-known role of Dsbs in the folding of secreted and cell envelope associated
283 proteins, we hypothesize that the effects on pathogenicity is the result of disruption in the stability
284 of unknown DsbA substrate(s). Our prior work established EntV as a DsbA substrate, currently
285 the only one identified (28). However, loss of EntV did not reduce pathogenicity in the worm model
286 (Figure 1A), and exposure to EntV, even at very high concentrations, was non-toxic to mammalian
287 cells (29). Thus, we do not favor EntV as being the source of DsbA's effects. A primary future
288 direction will be identifying additional substrates of DsbA and determining which contribute to
289 microlesion formation. Not only will this provide insight into the developmental requirements for
290 this cardiac pathology that promotes cardiomyocyte necroptosis, it will also impact understanding
291 of *E. faecalis* pathogenesis and the biology of disulfide bond forming proteins in bacteria.
292
293 Pneumococcal ChoP interactions with host PAFr were determined to be a prerequisite for
294 vascular endothelial cell invasion during IPD. In *S. pneumoniae*, the main wall teichoic acid chain
295 repeat is composed of 2-acetamido-4-amino-2,4,6-trideoxygalactose, glucose, ribitol-phosphate
296 and two GalNAc moieties, each decorated with phosphorylcholine. This cell wall teichoic acid
297 structure is considered rare and is thought to be exclusive to *S. pneumoniae* (47, 48). In light of
298 our observations of *E. faecalis* invasion of vascular endothelial cells despite an absence of this
299 wall teichoic acid structure, it is possible that another host receptor is required for endothelial cell
300 invasion. Interestingly, recent studies focused on bacterial cell wall entry and signaling in

301 eukaryotic cells have identified a PAFr-independent mechanism of tissue invasion that is actin-
302 dependent and engenders Rac1, Cdc42, and phosphatidylinositol 3-kinase (PI3K) signaling
303 leading to cell wall internalization via a macropinoctytosis-like pathway (49). Whether such a
304 pathway contributes to microlesion formation is unknown. In the future, it will be of interest to study
305 the mechanisms of tissue invasion and the host signaling pathways involved.
306
307 Cardiac microlesion formation is becoming increasingly appreciated as a risk factor during acute
308 infection (25), and this study establishes that *E. faecalis* is another etiological agent capable of
309 causing this pathology in a vertebrate animal model. There is an increased occurrence of heart
310 failure observed in patients with endocarditis (13-19), and we hypothesize that invasive infection
311 resulting in microlesions additionally occurs and is a contributing factor. It will be important to
312 investigate whether *E. faecalis* microlesions occur in humans and whether they contribute to
313 adverse cardiac events. As nosocomial derived enterococcal infections are increasingly
314 problematic among the elderly and immunocompromised patients (8-12), the development of
315 successful treatments will require identifying all disease manifestations as well as the bacterial
316 and the host factors involved.
317
318
319

320 **Methods and Materials**

321

322 ***C. elegans* survival assay**

323 *E. faecalis* strains were tested in *C. elegans* for survival as previously described (50). Briefly, *C.*
324 *elegans* strain N2 was maintained and propagated on *Escherichia coli* strain OP50 with standard
325 techniques. 30 *C. elegans* L4 nematodes were transferred from a lawn of *Escherichia coli* OP50
326 to a lawn of *E. faecalis* to be tested, incubated at 25°C, and examined at ≈24-hr intervals with a
327 dissecting microscope for viability. Worms were considered dead when they did not respond to
328 touch with a platinum wire pick. The data is representative of 3 independent experiments.
329 Nematode survival was plotted with the log-rank (Mantel-Cox) method using Prism 7 statistical
330 software (GraphPad).

331

332 **Bacterial strains and growth analysis**

333 All *E. faecalis* strains used in this project were used in previously published studies (28) and are
334 listed in Table S1. In a 96 well plate, overnight cultures (grown ~15 hours) of OG1RF strains were
335 diluted to an OD_{600nm} of 0.05 in brain heart infusion (BHI) agar medium (Difco) in a volume of
336 200µl / well in a 96-well plate. The 96-well plate containing the diluted cultures were then placed
337 in a prewarmed 37ºC BioTek Cytation 5 plate reader, and OD_{600nm} measurements were taken
338 every 10 minutes for 15 hours. Prior to measurement, the plate was gently agitated for 5 seconds.

339

340 **Mouse peritonitis and cardiac microlesion model**

341 The mouse peritonitis model was performed as described previously (51). The method for
342 identifying and evaluating cardiac microlesion formation was conducted as described previously
343 (20). Briefly, female, ~4 – 6-week old (~25g), ICR outbred mice were obtained from Envigo
344 (Indianapolis, Indiana) and were infected intraperitoneally with $7x10^8$ CFUs of *E. faecalis*. Mouse

345 hearts were obtained 24-48 hours post-infection, formalin fixed and sent to The University of
346 Texas Health Science Center Histopathology Laboratory for paraffin embedding, sectioning, and
347 hematoxylin and eosin H&E) staining. Paraffin embedded mouse hearts were first bisected and
348 sectioned longitudinally. 20 sections were cut per block, and every 5th section H&E stained in
349 order to measure the number and relative distribution of cardiac microlesions. Cardiac
350 microlesions were averaged across sections, and the differences between mouse groups
351 compared using *Student's* two-tailed t-test. Microlesions size measurements were also obtained
352 by measuring cardiac microlesion size on each section, and then averaging the values across
353 sections. ? Blinded reading? If so, might be worthwhile mentioning
354

355 **Necroptosis inhibition assay**

356 HL-1 cardiomyocytes were seeded in 24-well plates at a concentration of $5x10^5$ cells/ml. 24 hours
357 later, the cells were washed three times with Dulbecco's (1X) PBS, followed by pretreatment with
358 antibiotic free Claycomb medium supplemented with 10 μM of Necrostatin-1 (Sigma Aldrich),
359 GSK'872 (RD Systems), and Necrosulfonamaide (Millipore-Sigma) for 1 hour, followed by
360 infection at an MOI of 10 for 4 hours, following which the supernatant was collected, and
361 cytotoxicity in each well accessed using the CytoTox-ONE™ Homogeneous Membrane Integrity
362 Assay Kit (Promega). Each experiment was conducted in triplicate, on 3 separate occasions, and
363 averaged values between groups compared using using *Student's* two-tailed t-test.
364

365 **Annexin V apoptosis and necrosis assay.**

366 The annexin V apoptosis and necrosis assay was conducted using RealTime-Glo™ Annexin V
367 Apoptosis and Necrosis Assay Kit (Promega). The kit contains near-equimolar ratios of two
368 annexin V fusion proteins (Annexin V-LgBiT and Annexin V-SmBit) containing complementary
369 subunits of NanoBiT® Luciferase that, when combined following exposure to phosphatidyl serine,

370 results in an emission of a luminescent signal. The kit also contains a cell-impermeant
371 profluorescent DNA dye, which detects necrosis. Briefly, HL-1 cardiomyocytes (Sigma-Aldrich)
372 were seeded in a 96 well plate. 24 hours later, the cells were infected with *E. faecalis* at an MOI
373 = 50, in the presence of kit reagents. Luminescent and fluorescent readings were obtained every
374 30 minutes for up to 6 hours.
375
376 **Invasion assay**
377 SVEC4-10 Endothelial Cells (ATCC) were seeded in 24 well plates at a cell density of $1.5x10^5$
378 cells/ml. After 24 hours, the cells were washed three times with PBS, and infected with *E. faecalis*
379 at a MOI of 10 for 4 hours in antibiotic free Claycomb medium. After the incubation, the cells were
380 washed with Dulbecco's (1X) PBS three times and treated with trypsin, diluted in PBS, and plated
381 on BHI agar plates for attachment quantification. To measure intracellular numbers of *E. faecalis*,
382 cells that were washed three times with Dulbecco's (1X) PBS 4 h.p.i., then treated with Dulbecco's
383 Modified Eagle's Medium (ATCC) supplemented with 15 µg/ml vancomycin and 150 µg/ml
384 gentamicin. 24 hours later, the wells were washed three times with Dulbecco's (1X) PBS, lysed
385 using 0.1% Triton-X-100, and diluted and plated on BHI agar plates for intracellular quantification.
386 The ratio of invasion to attachment for a given enterococcal strain was used to calculate the
387 percent of invasion. The experiments were conducted on 3 independent occasions and were
388 performed using triplicate wells for each strain. Attachment and invasion values were averaged
389 from each experiment, and statistically analyzed using *Student's* two-tailed t-test.
390
391 **Cytotoxicity and inflammatory cytokine panel microtiter plate reader assay**
392 HL-1 cardiomyocytes were obtained from Sigma-Aldrich and SVEC4-10 Endothelial Cells were
393 obtained from ATCC. HL-1 cardiomyocytes (Sigma-Aldrich) were seeded into 24-well plates at a
394 concentration of $5x10^5$ cells/ml. 24 hours later, the cells were washed three times with Dulbecco's

395 (1X) PBS, and infected with *E. faecalis* at an MOI of 10 for 4 hours in antibiotic free Claycomb
396 medium. Supernatants were collected and centrifuged for 5 minutes at 10,000 G. Supernatant
397 was collected, and cytotoxicity assayed using CytoTox-ONE™ Homogeneous Membrane
398 Integrity Assay Kit (Promega). In addition to measuring cytotoxicity in HL-1 cardiomyocytes
399 infected with *E. faecalis* 4 h.p.i, inflammatory chemokines and cytokines were analyzed using a
400 Mouse Cytokine ELISA Plate Array III Colorimetric Assay (Signosis). The data represent an
401 average of at least 3 independent experiments for each isogenic mutant tested and were analyzed
402 using *Student's* two-tailed t-test.
403
404 **Immunofluorescence microscopy**
405 Immunofluorescence microcopy was conducted as described previously (20). Briefly, paraffin
406 embedded sections were treated with 1:100 rabbit Anti-mouse MLKL (phospho S345) antibody
407 [EPR9515(2)] in order to detect phosphorylated MLKL (Abcam), and 1:100 rat anti-mouse MLKL
408 antibody (Millipore-Sigma) for MLKL detection followed by treatment with 1:1000 chicken anti-
409 rabbit IgG (H+L) cross-adsorbed secondary Alexa Fluor 594 antibody (ThermoFisher), and 1:1000
410 goat anti-rat IgG (H+L) Secondary FITC Antibody (ThermoFisher) respectively. A rabbit anti-
411 *Enterococcus faecalis* antibody (Abcam) was used at a concentration of 1:1000 to detect *E.*
412 *faecalis* within cardiac microlesions followed by treatment with 1:1000 goat anti-rabbit IgG (H&L),
413 F(ab)'2 Fragment-affinity purified fluorescein (FITC) conjugate antibody (Invitrogen). All stained
414 sections were counterstained with 1:1000 DAPI (ThermoFisher) and mounted with Hardset™
415 Antifade Mounting Medium. Visualization of fluorescence was obtained using standard excitation
416 and emission wavelengths for Alexa 594, FITC, and DAPI on an Olympus FV3000RS high-speed
417 high-sensitivity inverted laser scanning confocal microscope.
418
419 **Generation of rabbit anti-DsbA antisera**

420 His-tagged recombinant DsbA was overexpressed in Rosetta-2(DE3) *E. coli* (Sigma-Aldrich) and
421 isolated by affinity purification via HisPur Nickel-NTA Resin (ThermoFisher) packed columns
422 followed by further purification and buffer exchange using Fast Protein Liquid Chromatography
423 (FPLC) to obtain highly pure samples of recombinant DsbA. The recovered recombinant protein
424 was then shipped to Cocalico Biologicals (Reamstown, PA) for generation of anti-DsbA antisera
425 through the immunization of rabbits. Throughout the immunization schedule, regular test bleeds
426 were performed and tested by Western blot using *E. faecalis* whole cell lysates and recombinant
427 DsbA in order to ensure the specificity of the rabbit anti-DsbA antisera.
428
429 ***E. faecalis* whole cell lysate and Western blot**
430 *E. faecalis* was grown overnight in 5 ml of BHI. The following day (~16 hours later), the media
431 was centrifuged at 6,738 G for 10 min at 4ºC. The pellet was resuspended in 5 ml of BHI, and
432 diluted 10X into fresh BHI media. The culture was subsequently incubated at 37ºC for an
433 additional 3.5 hours to obtain a culture of *E. faecalis* in exponential growth. The culture was then
434 spun down again at 6,738 G and supernatant removed. The pellet was then resuspended in 1ml
435 of ZAP buffer (10 mM Tris, 200 mM NaCl, pH 7.5) containing 1X protease inhibitor cocktail
436 (Roche) sonicated on ice with a max amplitude of 30%, and alternating on/off cycles consisting of
437 1 minute on, and 10 seconds off for a total of 5 minutes. Following sonication, the sample was
438 centrifuged at 10,000 G for 5 minutes and supernatant collected. The amount of protein in the
439 supernatant was quantified using a DC protein modified Bradford assay (BIORAD), and 10µg of
440 lysate was loaded in each lane of a 12% SDS-PAGE gel. Following electrophoresis and transfer
441 of protein to a PVDF membrane, the membrane was incubated overnight at 4ºC in a 5% milk
442 solution containing a 1:1000 dilution of rabbit anti-DsbA antisera followed by incubation with a
443 Goat anti-rabbit IgG HRP (ThermoFisher) secondary antibody at a dilution of 1:10,000 at room
444 temperature for 30 minutes prior to exposure.

Acknowledgements

This work was supported by the National Institute of Dental and Craniofacial Research of the National Institutes of Health under award numbers R01DE027608 to D. A. G. and F32DE027580 to A. O. B.

Table S1. Strains used in this study

***Enterococcus faecalis* Strains**				
Strain	**Genotype**	**Characteristics**	**Parent**	**Source**
OG1RF	Wild-type	Gel^+ Spr^+ Rf^R Fa^R	OG1	(52)
AOBD1	*ΔdsbA*	Gel^+ Spr^+ Rf^R Fa^R	OG1	(28)
AOBD2	*ΔdsbA::dsbA*	Gel^+ Spr^+ Rf^R Fa^R	OG1	(28)

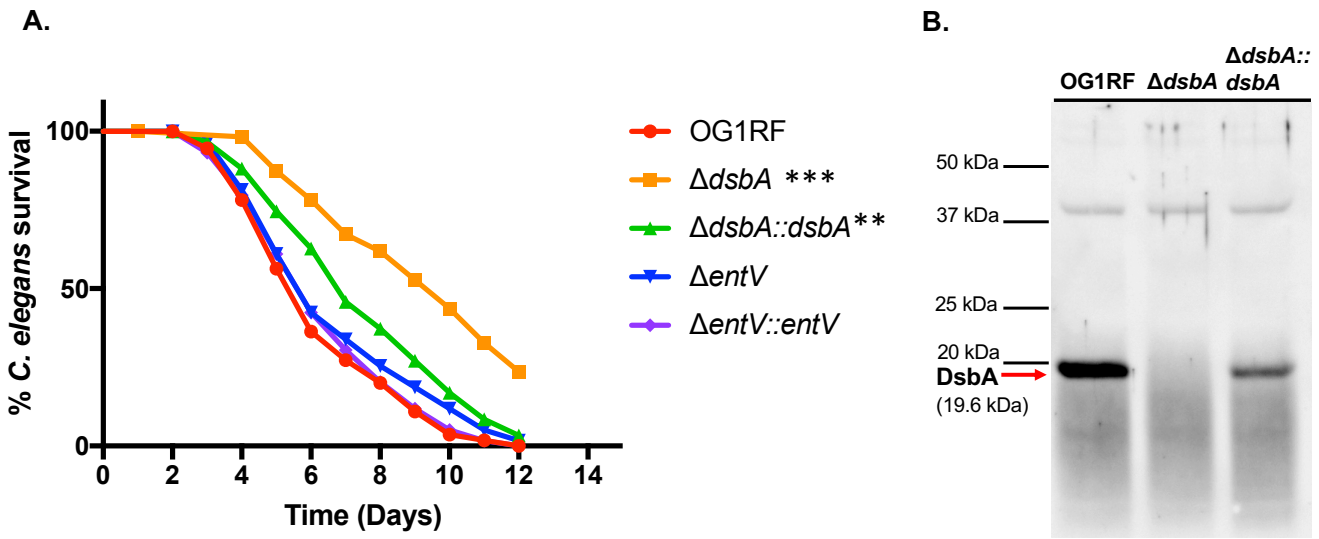

Figure 1. *dsbA* deficient *E. faecalis* show reduced virulence in a *C. elegans* survival assay. **(A)** L4 stage *C. elegans* were infected with *E. faecalis*. This figure is representative of 3 independent experiments with 30 worms/group. ****Asterisk indicate a $P < 0.0001$ and were analyzed by the log-rank (Mantel-Cox). **(B)** Western blot performed by SDS-PAGE separation of *E. faecalis* whole cell lysates followed by hybridization of DsbA using rabbit anti-DsbA antisera. Image is representative of 3 independent Western blot experiments.

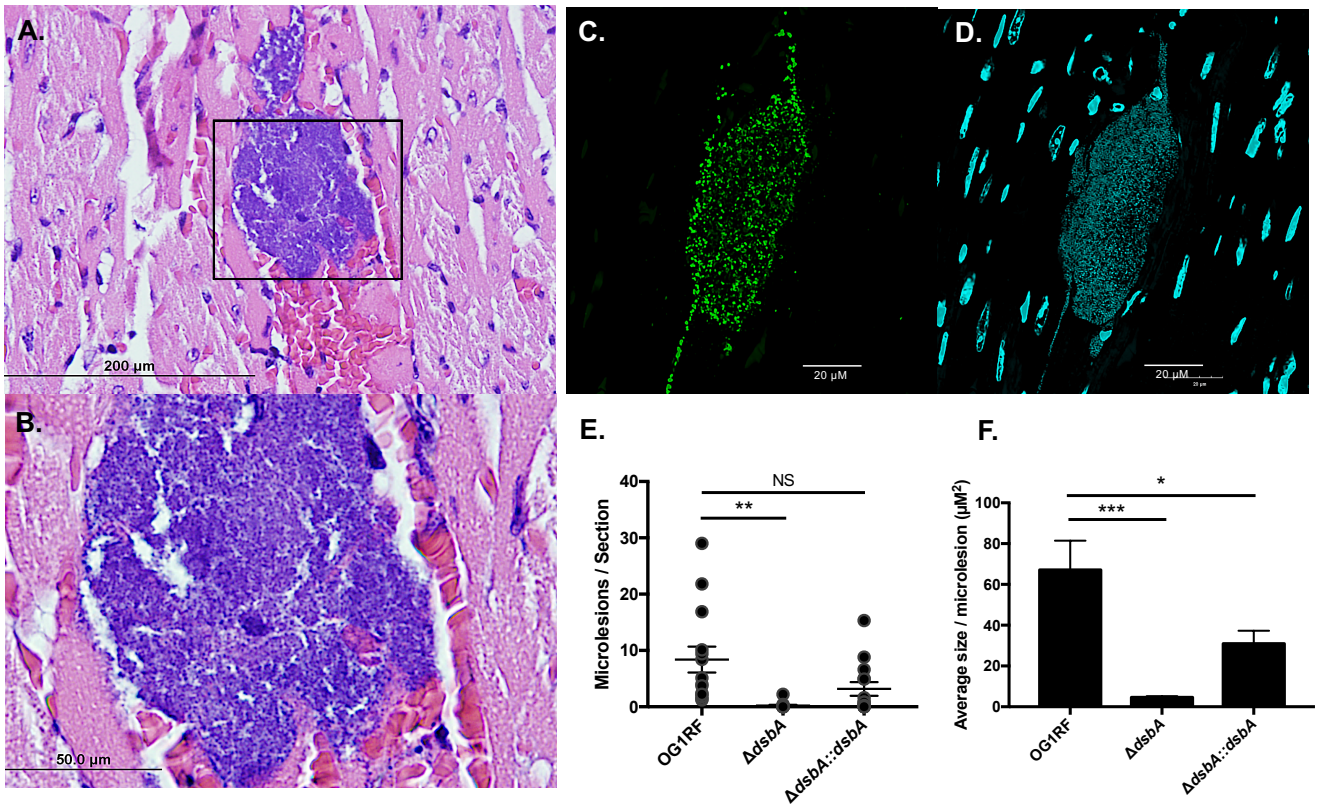

Figure 2. Cardiac microlesions form during invasive *E. faecalis* infection and are attenuated by loss of *dsbA*. Cardiac microlesions were observed using light microscopy of hematoxylin and eosin (H&E) stained paraffin embedded cardiac sections at 40X magnification **(A)**, and 100X magnification **(B)**. Immunofluorescent detection of *E. faecalis* was imaged using a 20X objective at 3X zoom (total of 60X magnification), a FITC conjugated anti-enterococcal antibody **(C)**, and DAPI for DNA staining **(D)**. Total microlesion counts **(E)**, and size measurements **(F)**, were obtained by quantification using light microscopy of H&E stained paraffin embedded cardiac sections from mice infected for 24-48 hours with *E. faecalis* (OG1RF n=14, Δ*dsbA* n=14, Δ*dsbA::dsbA* n=14). The data were averaged from 3 independent experiments, and analyzed using *Student's* two-tailed t-test (*** indicate a $P < 0.0001$).

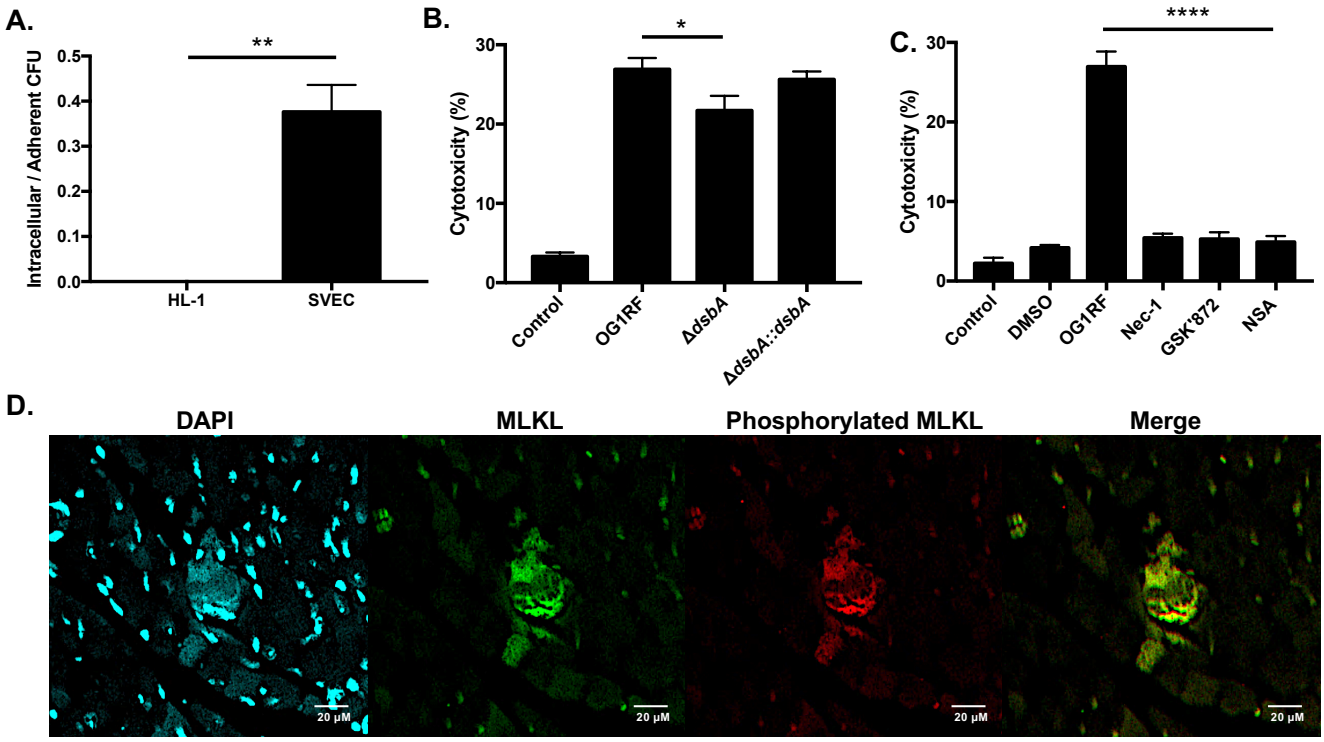

Figure 3. Necroptosis contributes to cardiotoxicity within cardiac microlesions. **(A)** Comparison of OG1RF invasion rates into HL-1 cardiomyocytes and SVEC endothelial cells. The graph represents data from 3 independent experiments that were analyzed using *Student's* two-tailed t-test (** indicate a $P < 0.01$). **(B)** *E. faecalis* induced cell death in HL-1 cardiomyocytes 4 hours post-infection (h.p.i.) as determined by measuring lactate dehydrogenase. The data represent an average of 3 independent experiments and were analyzed using *Student's* two-tailed t-test (* indicate a $P < 0.05$). **(C)** *E. faecalis* induced cell death in HL-1 cardiomyocytes 4 h.p.i. and was inhibited in the presence of inhibitors of necroptosis. The data represent an average of 3 independent experiments and were analyzed using *Student's* two-tailed t-test (**** indicate a $P < 0.0001$). **(D)** Immunofluorescent microscopy of paraffin embedded cardiac cross sections at 20X were performed to detect MLKL using FITC conjugated anti-MLKL antibodies, and Alexa 594 conjugated anti-phosphorylated MLKL antibodies at sites of microlesion formation, while DAPI was used to stain nuclei.

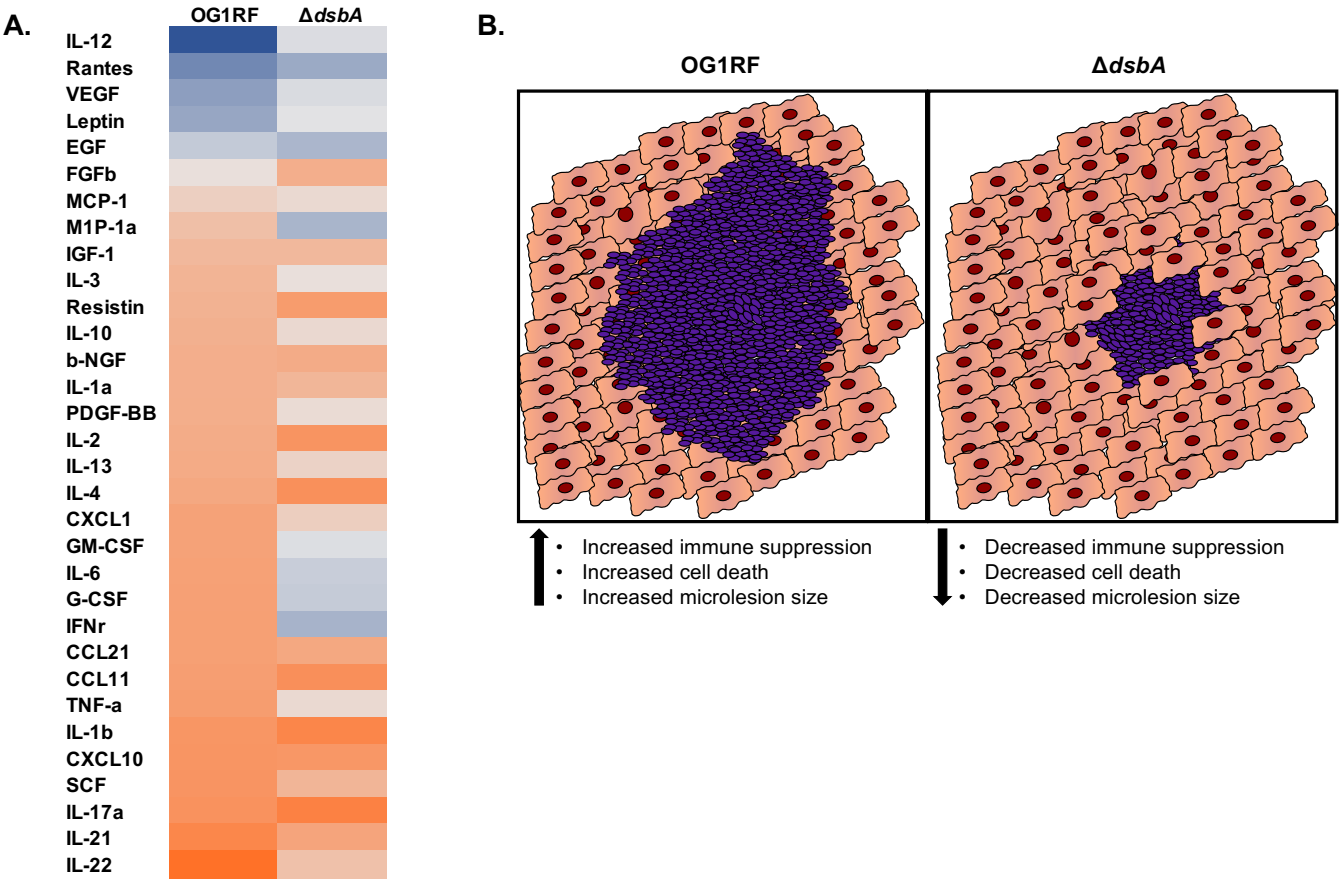

Figure 4. Wild-type *E. faecalis* suppresses the cardiomyocyte inflammatory response *in-vitro*. (A) HL-1 cardiomyocytes exposed to *E. faecalis* promote a suppressed inflammatory response while Δ*dsbA* infected cardiomyocytes yield a more inflammatory response. Data was obtained from the fold-expression change analysis (relative to uninfected controls) of at least 3 independent experiments for each strain. **(B)** Model of *E. faecalis* mediated suppression of the host cardiomyocyte immune response and effect on microlesion size.

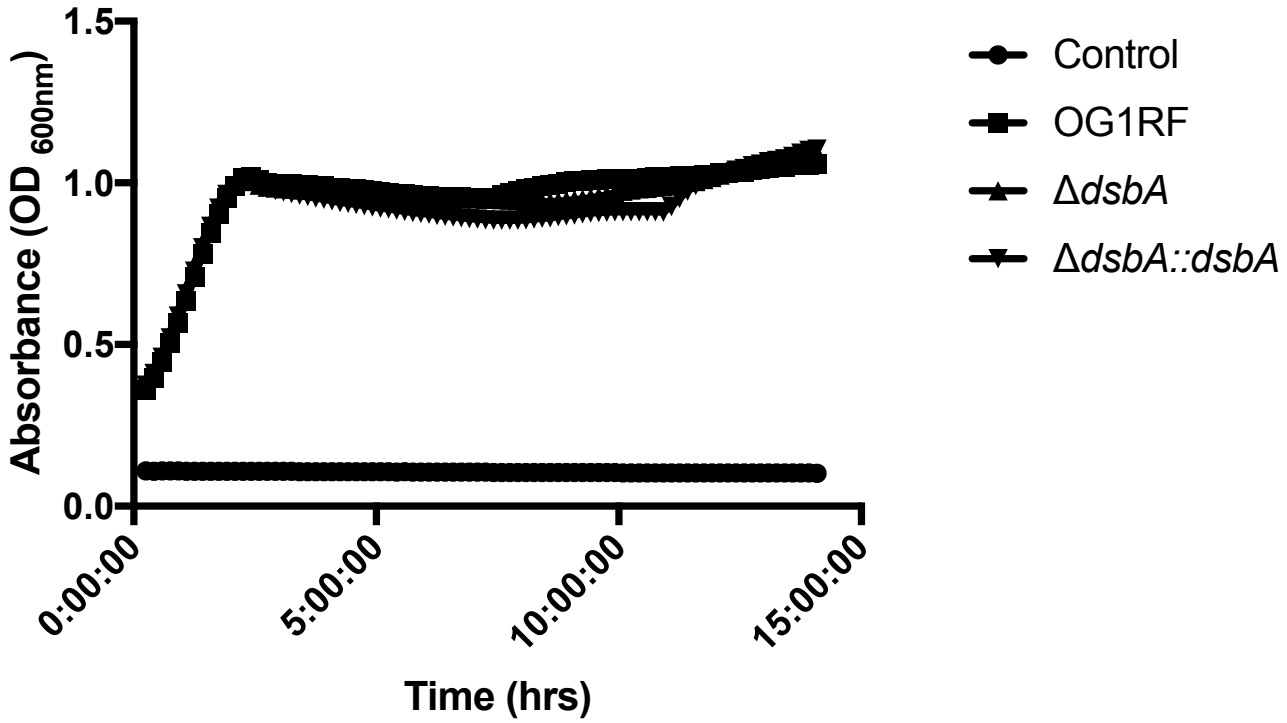

589
590
591
592
593
594
595
596
597
598
599
600
601
602
603
604
605
606
607
608
609
610
611
612
613
614
615
616
617

Supplemental Figure 1. *E. faecalis* growth curve. *E. faecalis* strains were grown for 15 hours in BHI and absorbance (OD_{600nm}) measured every 10 minutes. This figure is representative of 3 independent experiments.

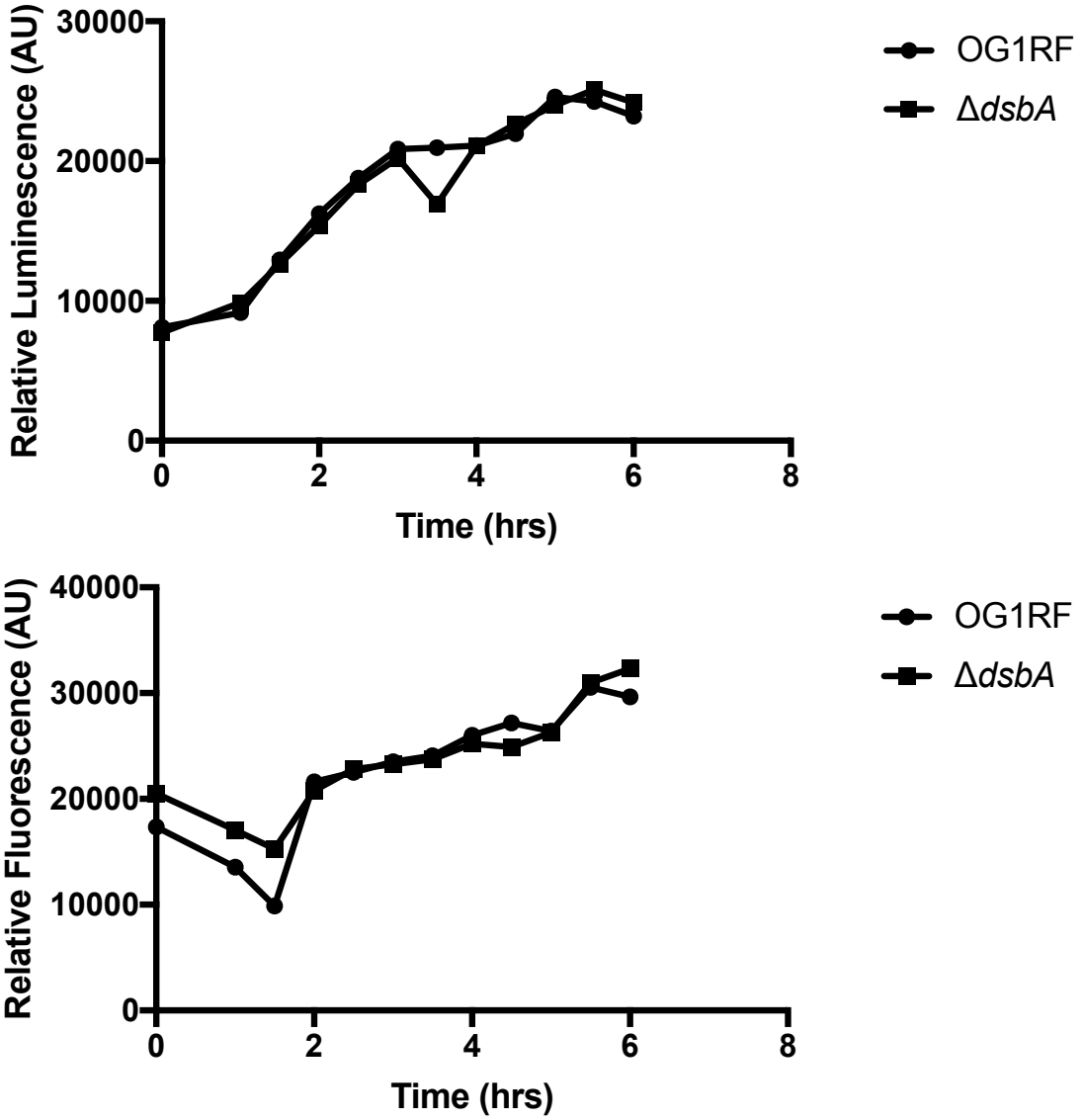

Supplemental Figure 2. Cardiomyocytes infected with *E. faecalis* die through an apoptosis independent mechanism. HL-1 cardiomyocytes were infected with *E. faecalis* at an MOI=50 for 4 hours in the presence of annexin V fusion proteins containing complimentary subunits of NanoBiT® Luciferase combined with a cell-impermeant profluorescent DNA dye to detect necrosis. A concomitant increase in both luminescent (apoptosis) **(A)** and fluorescent (necrosis) **(B)** signals are indicative of cell death through an apoptosis independent mechanism. The graphs represent an average of 3 independent experiments.

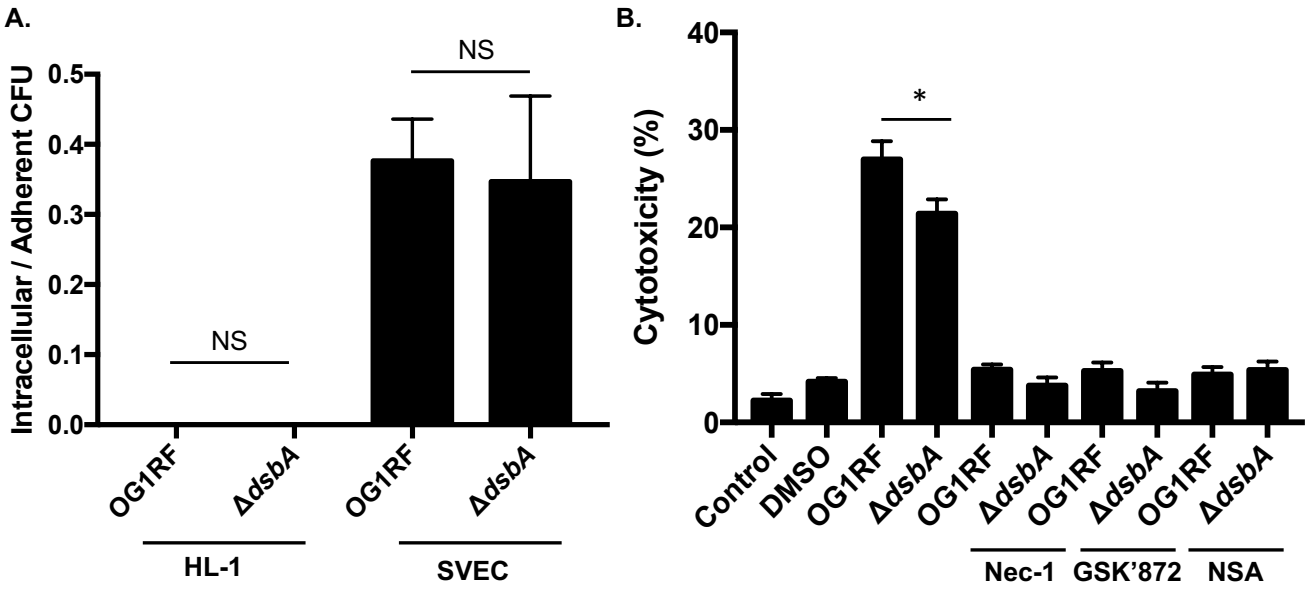

Supplemental Figure 3. Loss of *dsbA* does has no effect on endothelial cell invasion or necroptosis induced cell death of cardiomyocytes. (A) Comparison of WT and *ΔdsbA* invasion rates into HL-1 cardiomyocytes and SVEC endothelial cells showed no significant difference. The graph represents data from 3 independent experiments analyzed using *Student's* two-tailed t-test (NS denotes no significance). **(B)** Comparison of WT and *ΔdsbA* in HL-1 cardiomyocytes 4 h.p.i. in the presence of inhibitors of necroptosis *in-vitro* was determined by measuring lactate dehydrogenase. No significant difference was observed between necroptosis inhibitor conditions tested. The data represent an average of 3 independent experiments and were analyzed using *Student's* two-tailed t-test (* indicate a $P < 0.05$).

678 **References**

679

680 1. K. L. Frank *et al.*, Use of recombinase-based in vivo expression technology to characterize
681 Enterococcus faecalis gene expression during infection identifies in vivo-expressed
682 antisense RNAs and implicates the protease Eep in pathogenesis. *Infect Immun* **80**, 539-
683 549 (2012).

684 2. D. A. Garsin *et al.*, "Pathogenesis and Models of Enterococcal Infection" in Enterococci:
685 From Commensals to Leading Causes of Drug Resistant Infection, M. S. Gilmore, D. B.
686 Clewell, Y. Ike, N. Shankar, Eds. (Boston, 2014).

687 3. F. Lebreton, R. J. L. Willems, M. S. Gilmore, "Enterococcus Diversity, Origins in Nature,
688 and Gut Colonization" in Enterococci: From Commensals to Leading Causes of Drug
689 Resistant Infection, M. S. Gilmore, D. B. Clewell, Y. Ike, N. Shankar, Eds. (Boston, 2014).

690 4. H. S. Gold, Vancomycin-resistant enterococci: mechanisms and clinical observations. *Clin*
691 *Infect Dis* **33**, 210-219 (2001).

692 5. N. I. Agudelo Higuita, M. M. Huycke, "Enterococcal Disease, Epidemiology, and
693 Implications for Treatment" in Enterococci: From Commensals to Leading Causes of Drug
694 Resistant Infection, M. S. Gilmore, D. B. Clewell, Y. Ike, N. Shankar, Eds. (Boston, 2014).

695 6. M. Armstrong-Evans *et al.*, Control of transmission of vancomycin-resistant Enterococcus
696 faecium in a long-term-care facility. *Infect Control Hosp Epidemiol* **20**, 312-317 (1999).

697 7. H. M. S. Goh, M. H. A. Yong, K. K. L. Chong, K. A. Kline, Model systems for the study of
698 Enterococcal colonization and infection. *Virulence* **8**, 1525-1562 (2017).

699 8. L. M. Weiner *et al.*, Antimicrobial-Resistant Pathogens Associated With Healthcare-
700 Associated Infections: Summary of Data Reported to the National Healthcare Safety
701 Network at the Centers for Disease Control and Prevention, 2011-2014. *Infect Control*
702 *Hosp Epidemiol* **37**, 1288-1301 (2016).

703 9. K. C. Malani PN, Zervis MJ, *Enterococcal disease, epidemiology and treatment*, The
704 Enterococci: Pathogenesis, Molecular Biology and Antibiotic Resistance (ASM Press,
705 Washington, D.C., 2002).
706 10. H. Wisplinghoff *et al.*, Nosocomial bloodstream infections in US hospitals: analysis of
707 24,179 cases from a prospective nationwide surveillance study. *Clin Infect Dis* **39**, 309-317
708 (2004).
709 11. C. Chirouze *et al.*, Enterococcal endocarditis in the beginning of the 21st century: analysis
710 from the International Collaboration on Endocarditis-Prospective Cohort Study. *Clin*
711 *Microbiol Infect* **19**, 1140-1147 (2013).
712 12. J. R. McDonald *et al.*, Enterococcal endocarditis: 107 cases from the international
713 collaboration on endocarditis merged database. *Am J Med* **118**, 759-766 (2005).
714 13. C. H. Cabell *et al.*, Changing patient characteristics and the effect on mortality in
715 endocarditis. *Arch Intern Med* **162**, 90-94 (2002).
716 14. G. J. Garvey, H. C. Neu, Infective endocarditis--an evolving disease. A review of
717 endocarditis at the Columbia-Presbyterian Medical Center, 1968-1973. *Medicine*
718 *(Baltimore)* **57**, 105-127 (1978).
719 15. J. E. Geraci, W. J. Martin, Antibiotic therapy of bacterial endocarditis. VI. Subacute
720 enterococcal endocarditis; clinical, pathologic and therapeutic consideration of 33 cases.
721 *Circulation* **10**, 173-194 (1954).
722 16. E. Jawetz, M. Sonne, Penicillin-streptomycin treatment of enterococcal endocarditis. A re-
723 evaluation. *N Engl J Med* **274**, 710-715 (1966).
724 17. P. I. Lerner, L. Weinstein, Infective endocarditis in the antibiotic era. *N Engl J Med* **274**,
725 388-393 concl (1966).

726 18. L. Olaison, K. Schadewitz, E. Swedish Society of Infectious Diseases Quality Assurance
727 Study Group for, Enterococcal endocarditis in Sweden, 1995-1999: can shorter therapy
728 with aminoglycosides be used? *Clin Infect Dis* **34**, 159-166 (2002).
729 19. L. L. Pelletier, Jr., R. G. Petersdorf, Infective endocarditis: a review of 125 cases from the
730 University of Washington Hospitals, 1963-72. *Medicine (Baltimore)* **56**, 287-313 (1977).
731 20. A. O. Brown *et al.*, Streptococcus pneumoniae translocates into the myocardium and forms
732 unique microlesions that disrupt cardiac function. *PLoS Pathog* **10**, e1004383 (2014).
733 21. L. F. Reyes *et al.*, Severe Pneumococcal Pneumonia Causes Acute Cardiac Toxicity and
734 Subsequent Cardiac Remodeling. *Am J Respir Crit Care Med* **196**, 609-620 (2017).
735 22. A. T. Shenoy *et al.*, Streptococcus pneumoniae in the heart subvert the host response
736 through biofilm-mediated resident macrophage killing. *PLoS Pathog* **13**, e1006582 (2017).
737 23. T. Brissac, A. T. Shenoy, L. A. Patterson, C. J. Orihuela, Cell Invasion and Pyruvate
738 Oxidase-Derived H2O2 Are Critical for Streptococcus pneumoniae-Mediated
739 Cardiomyocyte Killing. *Infect Immun* **86** (2018).
740 24. A. T. Shenoy, C. J. Orihuela, Anatomical site-specific contributions of pneumococcal
741 virulence determinants. *Pneumonia (Nathan)* **8** (2016).
742 25. D. M. Musher, M. S. Abers, V. F. Corrales-Medina, Acute Infection and Myocardial
743 Infarction. *N Engl J Med* **380**, 171-176 (2019).
744 26. V. F. Corrales-Medina *et al.*, Association between hospitalization for pneumonia and
745 subsequent risk of cardiovascular disease. *JAMA* **313**, 264-274 (2015).
746 27. S. R. Jafarzadeh, B. S. Thomas, D. K. Warren, J. Gill, V. J. Fraser, Longitudinal Study of
747 the Effects of Bacteremia and Sepsis on 5-year Risk of Cardiovascular Events. *Clin Infect*
748 *Dis* **63**, 495-500 (2016).

749 28. C. E. G. Armand O. Brown, Melissa R. Cruz, Michael C. Lorenz, Danielle A. Garsin,
750 Antifungal activity of the Enterococcus faecalis peptide EntV requires protease cleavage
751 and disulfide bond formation. *Mbio* **10**, 1-13 (2019).
752 29. C. E. Graham, M. R. Cruz, D. A. Garsin, M. C. Lorenz, Enterococcus faecalis bacteriocin
753 EntV inhibits hyphal morphogenesis, biofilm formation, and virulence of Candida albicans.
754 *Proc Natl Acad Sci U S A* **114**, 4507-4512 (2017).
755 30. R. P. Gilley *et al.*, Infiltrated Macrophages Die of Pneumolysin-Mediated Necroptosis
756 following Pneumococcal Myocardial Invasion. *Infect Immun* **84**, 1457-1469 (2016).
757 31. T. Zhang *et al.*, CaMKII is a RIP3 substrate mediating ischemia- and oxidative stress-
758 induced myocardial necroptosis. *Nat Med* **22**, 175-182 (2016).
759 32. A. Linkermann *et al.*, Necroptosis in immunity and ischemia-reperfusion injury. *Am J*
760 *Transplant* **13**, 2797-2804 (2013).
761 33. A. Linkermann *et al.*, Two independent pathways of regulated necrosis mediate ischemia-
762 reperfusion injury. *Proc Natl Acad Sci U S A* **110**, 12024-12029 (2013).
763 34. K. Kitur *et al.*, Necroptosis Promotes Staphylococcus aureus Clearance by Inhibiting
764 Excessive Inflammatory Signaling. *Cell Rep* **16**, 2219-2230 (2016).
765 35. F. J. Ramos Tuarez, M. A. Law, "Cardiac Abscess" in StatPearls. (Treasure Island (FL),
766 2019).
767 36. C. R. Gentry-Weeks, R. Karkhoff-Schweizer, A. Pikis, M. Estay, J. M. Keith, Survival of
768 Enterococcus faecalis in mouse peritoneal macrophages. *Infect Immun* **67**, 2160-2165
769 (1999).
770 37. J. Zou, N. Shankar, Enterococcus faecalis infection activates phosphatidylinositol 3-kinase
771 signaling to block apoptotic cell death in macrophages. *Infect Immun* **82**, 5132-5142
772 (2014).

773 38. J. Zou, N. Shankar, The opportunistic pathogen Enterococcus faecalis resists phagosome
774 acidification and autophagy to promote intracellular survival in macrophages. *Cell Microbiol*
775 **18**, 831-843 (2016).
776 39. K. V. Singh, S. L. La Rosa, S. R. Somarajan, J. H. Roh, B. E. Murray, The fibronectin-
777 binding protein EfbA contributes to pathogenesis and protects against infective
778 endocarditis caused by Enterococcus faecalis. *Infect Immun* **83**, 4487-4494 (2015).
779 40. S. R. Nallapareddy, X. Qin, G. M. Weinstock, M. Hook, B. E. Murray, Enterococcus faecalis
780 adhesin, ace, mediates attachment to extracellular matrix proteins collagen type IV and
781 laminin as well as collagen type I. *Infect Immun* **68**, 5218-5224 (2000).
782 41. S. R. Nallapareddy *et al.*, Endocarditis and biofilm-associated pili of Enterococcus faecalis.
783 *J Clin Invest* **116**, 2799-2807 (2006).
784 42. M. E. Reardon-Robinson, H. Ton-That, Disulfide-Bond-Forming Pathways in Gram-
785 Positive Bacteria. *J Bacteriol* **198**, 746-754 (2015).
786 43. C. Landeta, D. Boyd, J. Beckwith, Disulfide bond formation in prokaryotes. *Nat Microbiol*
787 **3**, 270-280 (2018).
788 44. R. Daniels *et al.*, Disulfide bond formation and cysteine exclusion in gram-positive bacteria.
789 *J Biol Chem* **285**, 3300-3309 (2010).
790 45. R. J. Dutton, D. Boyd, M. Berkmen, J. Beckwith, Bacterial species exhibit diversity in their
791 mechanisms and capacity for protein disulfide bond formation. *Proc Natl Acad Sci U S A*
792 **105**, 11933-11938 (2008).
793 46. A. Dumoulin, U. Grauschopf, M. Bischoff, L. Thony-Meyer, B. Berger-Bachi,
794 Staphylococcus aureus DsbA is a membrane-bound lipoprotein with thiol-disulfide
795 oxidoreductase activity. *Arch Microbiol* **184**, 117-128 (2005).

796 47. D. Denapaite, R. Bruckner, R. Hakenbeck, W. Vollmer, Biosynthesis of teichoic acids in
797 Streptococcus pneumoniae and closely related species: lessons from genomes. *Microb*
798 *Drug Resist* **18**, 344-358 (2012).
799 48. W. Fischer, T. Behr, R. Hartmann, J. Peter-Katalinic, H. Egge, Teichoic acid and
800 lipoteichoic acid of Streptococcus pneumoniae possess identical chain structures. A
801 reinvestigation of teichoid acid (C polysaccharide). *Eur J Biochem* **215**, 851-857 (1993).
802 49. L. N. Loh, G. Gao, E. I. Tuomanen, Dissecting Bacterial Cell Wall Entry and Signaling in
803 Eukaryotic Cells: an Actin-Dependent Pathway Parallels Platelet-Activating Factor
804 Receptor-Mediated Endocytosis. *MBio* **8** (2017).
805 50. D. A. Garsin *et al.*, A simple model host for identifying Gram-positive virulence factors. *Proc*
806 *Natl Acad Sci U S A* **98**, 10892-10897 (2001).
807 51. K. V. Singh, X. Qin, G. M. Weinstock, B. E. Murray, Generation and testing of mutants of
808 Enterococcus faecalis in a mouse peritonitis model. *J Infect Dis* **178**, 1416-1420 (1998).
809 52. B. E. Murray *et al.*, Generation of restriction map of Enterococcus faecalis OG1 and
810 investigation of growth requirements and regions encoding biosynthetic function. *J*
811 *Bacteriol* **175**, 5216-5223 (1993).
812
813
814